Supporting Information

Study of Depth and Size of Concave Cube Au Nanoparticles as Highly Sensitive SERS Probes

José M. Romo-Herrera[*,†], *Ana L. González*[▪], *Luca Guerrini*[⏥,‡], *Francisco R. Castiello*[†], *Gabriel Alonso-Núñez*[†], *Oscar E. Contreras*[†] *and Ramón A. Alvarez-Puebla*[⏥,▲].

† Centro de Nanociencias y Nanotecnología, UNAM, Ensenada B.C., C.P. 22800, México. ▪ Instituto de Física, Benemérita Universidad Autónoma de Puebla, Apartado Postal J48, 72570 Puebla, México. ⏥ Universitat Rovira i Virgili. C/ Marcel•lí Domingo s/n, 43007 Tarragona, Spain. ‡ Medcom Advance SA. Viladecans Bussines Park, Edificio Brasil, C/Bertran i Musitu, 83-85, 08840 Viladecans (Barcelona), Spain. ▲ ICREA. Passeig Lluís Companys 23, 08010 Barcelona, Spain.

*Address correspondence to: jmromo@cnyn.unam.mx

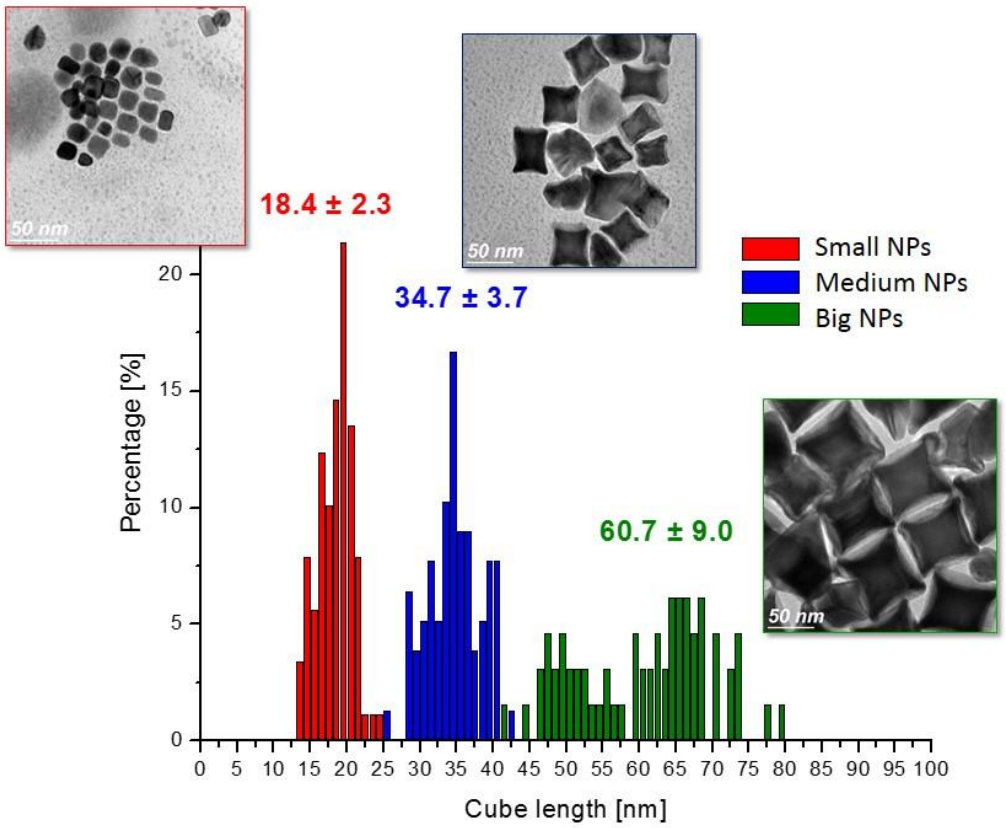

Figure SI-1. Size statistics from the three different colloid samples obtained, resulting in a mean size per sample. The measurements were done from TEM pictures, measuring the side length of the concave cubes.

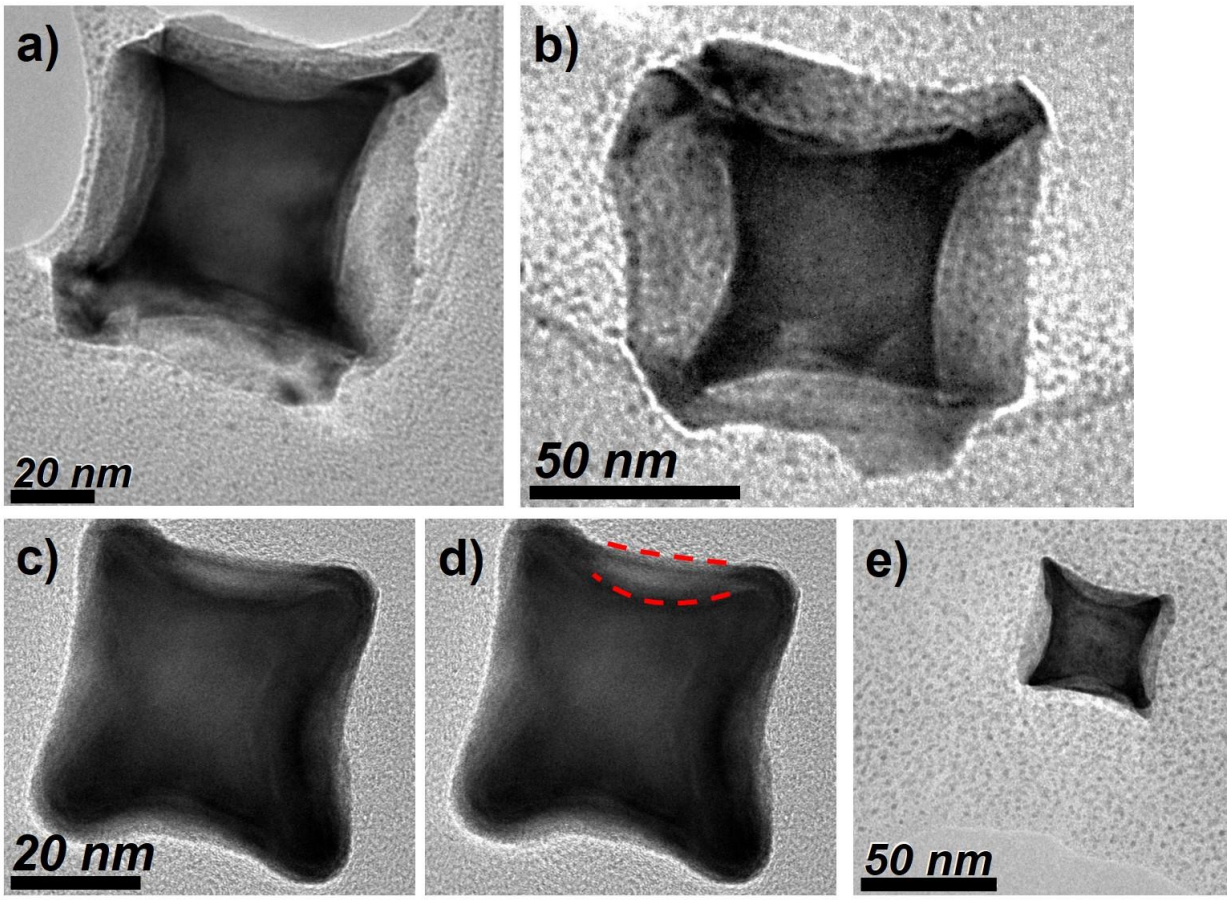

Figure SI-2. TEM images from different perspectives of the concave cube morphology exploring the shape of the nanocubes, with special emphasis on the edges of the nanocubes. Figure SI-2a and Figure SI-2b present two different nanocubes with some inclination degree that enables to perceive a perspective showing the edges of the cube from where it can be seen edges very close to straight. Figure SI-2c shows a different nanocube with a frontal view where different contrast lines can be observed (contrast lines associated to the mass thickness of the nanoparticle); in Figure SI-2d the lower red dashed line is marking the change from the darkest contrast to the brighter zone with a well-defined degree of curvature which we assign to the concavity, but the upper red dashed line shows a line with a slightly curved edge of the nanocube. In Figure SI-2e we display another typical nanocube showing again the change in contrast next to the edge, with an almost straight edge as the final line in the outline of the nanoparticle. This type of observation drive us to think that most of the nanocubes are presenting cube edges very close to straight.

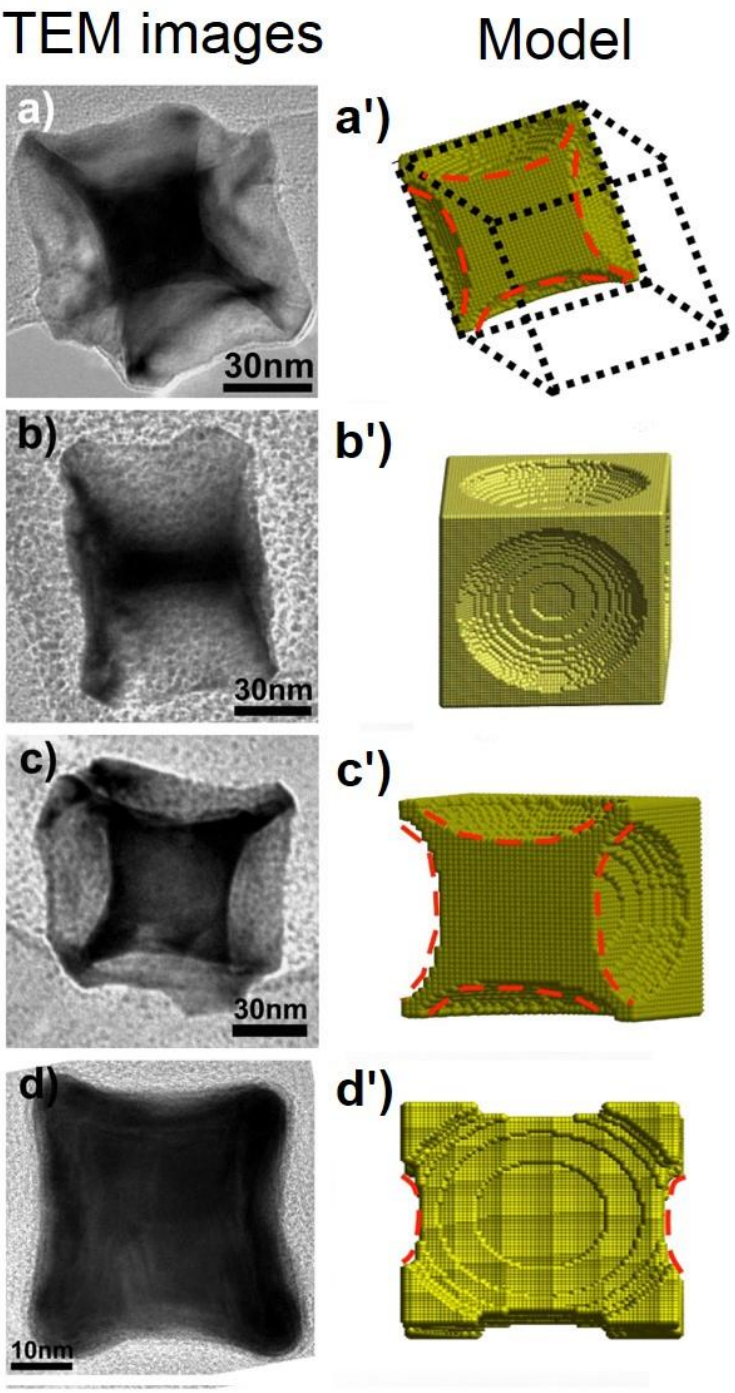

Figure SI-3. TEM images from different perspectives of the NPs, next to illustrative models to show the morphology of the concave cubes Au nanoparticles. The perspectives observed in Figure SI-3a, SI-3b and SI-3c allow to suppose that the edges of the nanocubes tend to be very close to straight. Figure SI-3a´, SI-3b´ and SI-3c´ are the models of the concave nanocubes with straight edges. Figure SI-3d and SI-3d´ present TEM and model images of a different nanocube where slightly curved edges are observed.

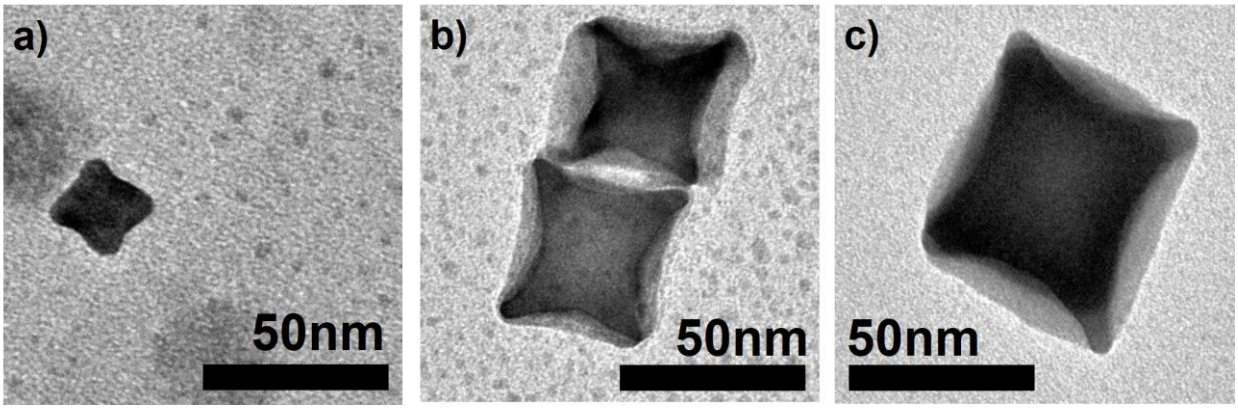

Figure SI-4. Comparison of representative nanocubes of the three different samples (small, medium and big-GNC). The images observation allow us to think that a tendency of the depth of the concavities of the GNCs as a function of the size of the nanocubes exist. This is based in the degree of curvature from the darkest constrast zone (constrast that is associate to the mass thickness of the sample) from where the tendency can be inferred.

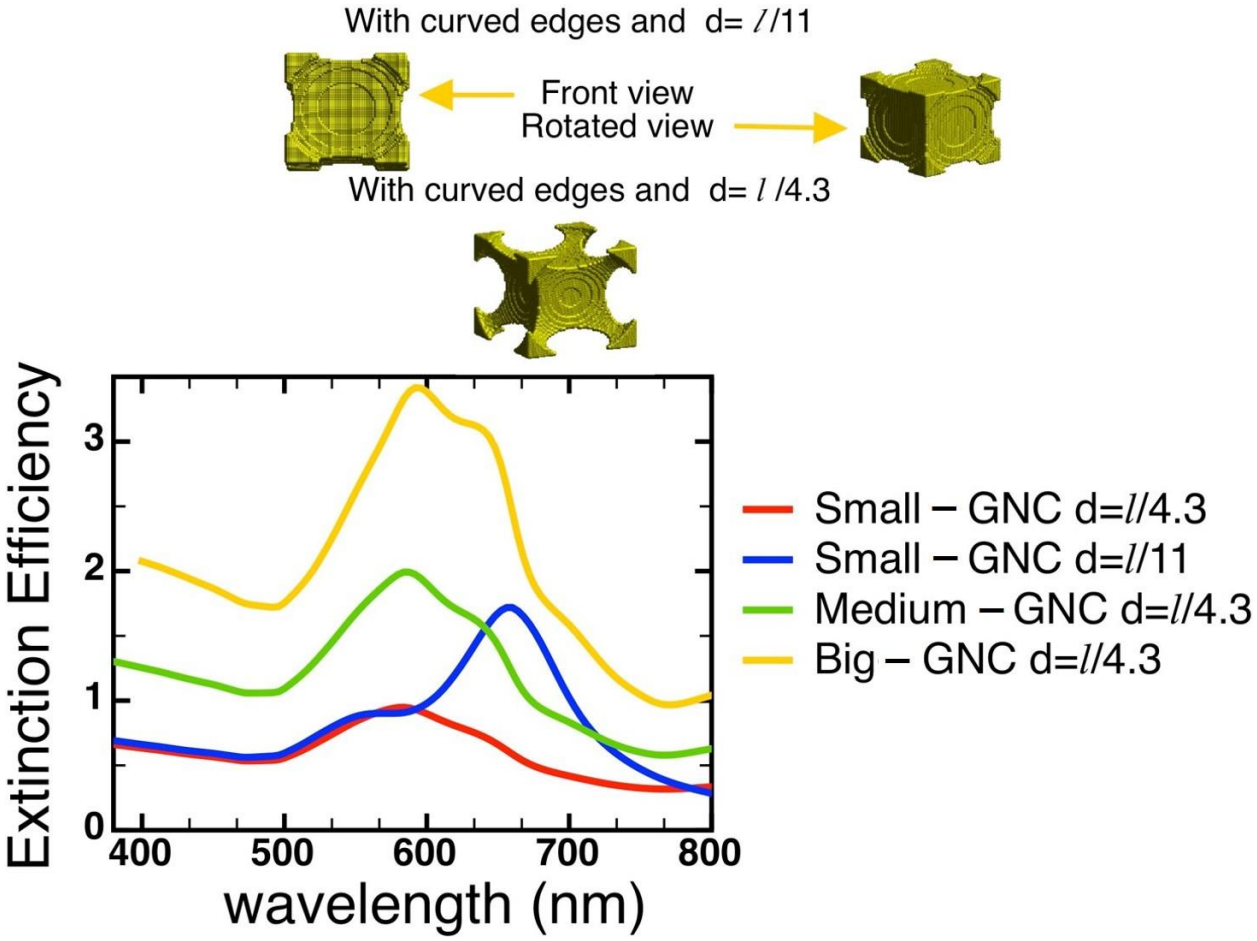

Figure SI-5. Calculated optical response of small, medium and big GNCs with a morphology represented by the ***curved edges cube*** model with different values of "*d*", being this the degree of the concavity in terms of the length side "*l*" of the cube. The spectra were calculated using an array of dipoles of the order of 10^5 to guarantee convergence in the results. Due to the symmetry of the nanoparticle only one configuration has been calculated. The incident field is parallel to a face and the wave vector is perpendicular to it. This morphology was discarded as the predominant due to its discrepancy with the experimental spectra.

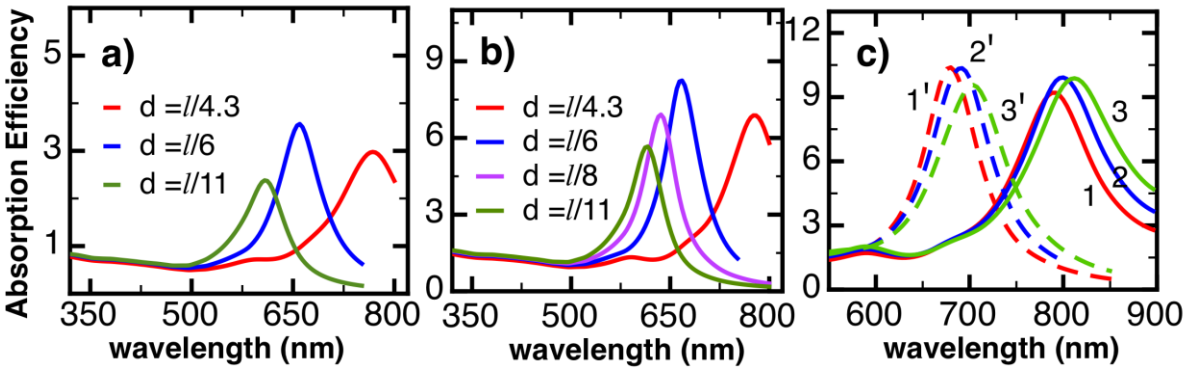

LSPR behavior as a function of the degree of concavity.

Figure SI-6. Simulated optical absorption spectra of a) small (*l*= 18 nm), b) medium (*l* = 35 nm) and c) large (*l* = 50, 60, 70 nm) GNCs and considering various values of profundity of the concavity, "d". In c) line 1, 2 and 3 correspond to a value of d = *l*/4.3 and *l* = 50, 60, 70 nm, respectively; 1', 2' and 3' for a value of d=*l*/6.

Small GNCs with d = *l*/4.3, *l*/6, *l*/11 show LSPRs located at 768 nm, 660 nm and 608 nm, respectively. LSPRs of medium-GNCs with d = *l*/4.3, *l*/6, *l*/8, *l*/11 are centered at 776 nm, 668 nm, 636 nm, 616 nm. For big-GNCs, the positions of the LSPR are 792nm (line 1), 800 nm (line 2), 812 (line 3), 680 nm (line 1'), 692 nm (line 2'), 704 nm.

From this analysis we conclude that despite the wide size statistic in sample of big-GNCs the average size of 60 nm is representative of the sample. Besides, the concavity of the cube plays an important role in the position of the LSPR. In all the cases we have observed the same trend, as the concavity becomes deeper, the LSPR red-shifts.

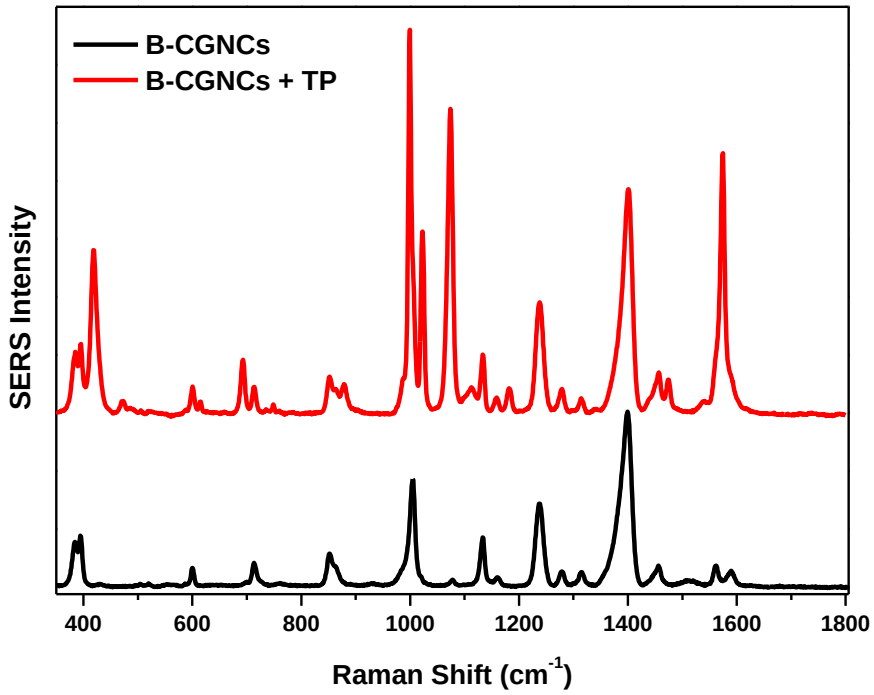

Figure SI-7 Baseline corrected SERS spectrum of TP on big-GNCs (red curve) and background SERS spectrum of big-GNCs (black curve).

SERS Enhancement Factor

The SERS enhancement factor was calculated according to the following formula [A]:

$$EF = \frac{I_{SERS} / N_{Surf}}{I_{Raman} / N_{Vol}}$$

where N_{Vol} is the average number of molecules in the scattering volume, V, for the normal Raman measurement, and N_{Surf} is the average number of adsorbed molecules in the same scattering volume for the SERS measurement. As normal Raman and SERS intensities (I_{Raman} and I_{SERS}) we selected the height of the band at ca. 1074 cm^{-1}. Both Raman and SERS measurements were performed under the same experimental set-up (i.e. identical scattering volume).

We then assumed that all TP molecules added to the GNC suspension attached to the metallic surface (final concentration in the sample equals to 8.5×10^{-6} M). Thus, by comparison of the intensity of the SERS spectra (number of TP moles adsorbed onto 1 L of colloidal dispersions = 8.5×10^{-6} M) to the intensity of the normal Raman spectra of a TP 98% solution (9.74 M), we can then calculate the EFs at different excitation wavelengths.

References

[A] E. C. Le Ru and P. G. Etchegoin, *Principles of Surface-Enhanced Raman Spectroscopy*, 2009. Elsevier Ed. ISBN: 978-0-444-52779-0